

Magnetoresistive behavior and magnetization reversal of NiFe/Cu/CoFe/IrMn spin valve GMRs in nanoscale

Cong Yin, Ze Jia, Wei-chao Ma, and Tian-ling Ren

Institute of Microelectronics & Tsinghua National Laboratory for Information Science and Technology, Tsinghua University, Beijing 100084, China

(Received: 13 September 2012; revised: 8 January 2013; accepted: 11 January 2013)

Abstract: The magnetoresistance behavior and the magnetization reversal mode of NiFe/Cu/CoFe/IrMn spin valve giant magnetoresistance (SV-GMR) in nanoscale were investigated experimentally and theoretically by nanosized magnetic simulation methods. Based on the Landau-Lifshitz-Gilbert equation, a model with a special gridding was proposed to calculate the giant magnetoresistance ratio (MR) and investigate the magnetization reversal mode. The relationship between MR and the external magnetic field was obtained and analyzed. Studies into the variation of the magnetization distribution reveal that the magnetization reversal mode, that is, the jump variation mode for NiFe/Cu/CoFe/IrMn, depends greatly on the antiferromagnetic coupling behavior between the pinned layer and the antiferromagnetic layer. It is also found that the switching field is almost linear with the exchange coefficient.

Keywords: giant magnetoresistance (GMR); spin valves; nanoscale; magnetization reversal

1. Introduction

With the discovery of the giant magnetoresistance (GMR) effect [1] and spin valve (SV) GMR [2], SV-GMRs have been extensively studied both for their potential application and for their scientific interest in nanoscale due to their high sensitivity, scalability, and no interference of the background magnetic signal. Different micro-sized SV-GMR structures have been fabricated and studied with different stacks, such as Ta/NiFe/Co/Cu/Co/NiFe/FeMn/Ta and Ta/NiFe/Cu/CoFe/PtMn/Ta [3-6]; the micromagnetic simulation of GMR structures, such as the simulation of the transfer curve in the GMR head and that of the domain wall displacement [7-10], also attracted attention due to its guidance for researchers. However, with the scaling down of novel GMR devices, it is valuable to investigate the magnetic properties of nanosized SV-GMRs for further application. Therefore, the magnetization reversal mode and magnetoresistive behavior in SV-GMR were investigated through magnetoresistance experiments and the developed nanosized magnetic simulation method in the study.

A SV-GMR sample was fabricated and the magnetic

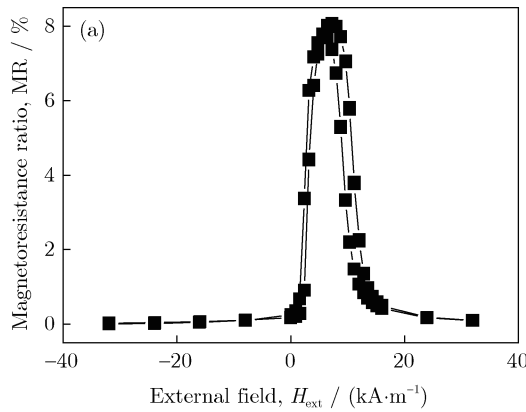
and structural characteristics were carefully investigated, which were described in Section 2. The nanosized magnetic theory was described, and the model based on the SV stack and Stoner-Wohlfarth model [11] was developed and extended to obtain the magnetoresistance ratio (MR) in Section 3, in which both the detailed nanosized structure and magnetization distribution were taken into account. The MR value of the NiFe/Cu/CoFe/IrMn stack in nanoscale was studied in Section 4.1. The magnetization reversal mode and the influencing factor of the exchange coefficient were investigated in Section 4.2.

2. Experimental

Ta (3)/NiFe (4.5)/CoFe (1)/Cu (1.8)/CoFe (3.5)/IrMn (11)/Ta (3) (in nm) (Ni81Fe19, at%; Co90Fe10, at%; Ir19Mn81, at%) was deposited by dc-magnetron sputtering on Si (100) substrates with the 100 nm SiO₂ layer (Fig. 1) in a vacuum system with a backing pressure below 2×10^{-6} Pa. A magnetic field of 7.96 kA/m was applied parallel to the substrates during the sputtering. The structures were subsequently annealed at a magnetic field of 79.6 kA/m at 260°C in vacuum for 1 h. The bottom Ta serves as

a buffer layer which is helpful for the crystal orientations of the upper NiFe and CoFe while the top Ta serves as a capping layer protecting the films below it. MR was measured by the standard four-probe measurement method at room temperature (RT). Atomic force microscopy (AFM) was presented to investigate the root-mean-square (RMS) surface roughness and the crystal structure of the spin valve film.

It can be seen in Fig. 2(a) that MR is 8.1% at room temperature when the external field and the exchange biasing field were both in the width direction. Close-packed spherical grains and a smooth, dense, and uniform surface can be found in the sample with the RMS surface roughness of 0.27 nm, which is far less than the whole film thickness, as shown in Fig. 2(b). Since the grain size is an important factor to the MR value, the coercive field, the exchange biasing field, and the spin-dependent scattering



properties of SV-GMRs, as proofed by Ref. [12], the vacuum and the precise control of the thickness of every layer are absolutely crucial.

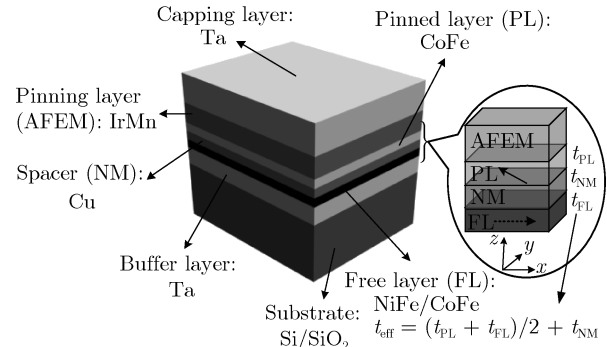


Fig. 1. Schematic diagram of the SV-GMR and the simulated FL/NM/PL/AFEM model.

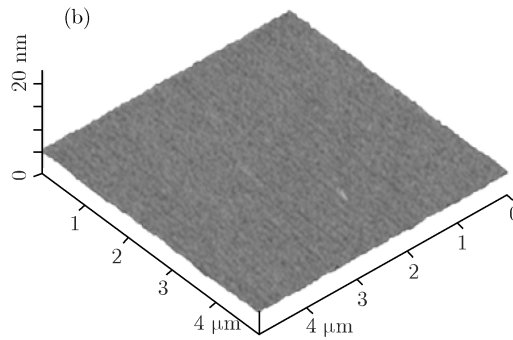


Fig. 2. Dependence of the magnetoresistance ratio MR on the external field H_{ext} (a) and $5 \mu\text{m} \times 5 \mu\text{m}$ AFM image (b).

3. Theoretical approaches

A three-dimensional model has been developed to study the SV-GMRs. A basic spin valve stack (Fig. 1) is composed of an antiferromagnetic pinning layer (AFEM), a ferromagnetic pinned layer (PL), a nonmagnetic metal spacer layer (NM), and a ferromagnetic free layer (FL). Ta is not included in the model because it is supposed that the crystal orientation of the ferromagnetic layer is not considered here. The nanosized magnetic theory and the MR calculation are introduced as follows.

3.1. Nanosized magnetic simulation model

The simulation is based on the nanosized magnetic theory, assuming that the magnetization \vec{M} is a continuous function on positions at a given temperature, and the whole magnetization is kept unchanged [12-14]. The finite difference method is adopted by the object oriented micromagnetic framework (OOMMF) software [13] to calculate the Landau-Lifshitz-Gilbert equation [15], which is expressed by

$$d\vec{M}/dt = -|\vec{r}|\vec{M} \times \vec{H}_{eff} - (|\vec{r}|\alpha/M_s)\vec{M} \times (\vec{M} \times \vec{H}_{eff}) \quad (1)$$

where \vec{r} is the Landau-Lifshitz gyromagnetic ratio, \vec{H}_{eff} is the effective magnetic field, M_s is the saturation magnetization, and α is the damping constant that determines the rate of the energy dissipation. The study of SV structure is also based on the Stoner-Wohlfarth model [11], which assumes that the magnetizations of ferromagnetic layers rotate continuously.

In the experiment, the spin valve is NiFe/CoFe/Cu/CoFe/IrMn structure, in which NiFe/CoFe acts as the free layer due to the trade-off of the coercive field and the magnetoresistance ratio. To simplify the simulation process, only NiFe was used as the free layer, that is, NiFe/Cu/CoFe/IrMn structure was adopted as the model. The hard axis and the easy axis were in the x and y directions, respectively. The planar dimension was set at $500 \text{ nm} \times 50 \text{ nm}$ to achieve good shape anisotropy [14]. The thicknesses of NiFe/Cu/CoFe were $3 \text{ nm}/2 \text{ nm}/3 \text{ nm}$. An equivalent magnetic field \vec{H}_{bias} in the easy axis direction

was used in the simulation to equal the pinning field, that is, the exchange biasing field between the antiferromagnetic metal IrMn layer and pinned layer. Other parameters of Co₉₀Fe₁₀ and Ni₈₁Fe₁₉ were presented in Table 1, where A is the exchange constant and K_1 is the magnetocrystalline anisotropy constant in the ferromagnetic metals.

Table 1. Parameters of different materials of SV-GMRs

Material	$M_s / (\text{A}\cdot\text{m}^{-1})$	$A / (\text{J}\cdot\text{m}^{-1})$	$K_1 / (\text{J}\cdot\text{m}^{-3})$
NiFe	8.6×10^5	1.3×10^{-11}	0
CoFe	1.43×10^6	2.91×10^{-11}	4.73×10^5

3.2. Giant magnetoresistance calculation

The GMR resistance calculation was presented in this part. The calculation method was extended from the calculation method of the Co-AMR nanostructure [16]. The inhomogeneities of the magnetization distribution should be considered when calculating MR of the GMR nanostructure [16-17]. Thus, the spin valve structure was divided into lines in length, and each line with cells in the cross section (width and thickness plane). The cell was set to be $5 \text{ nm} \times 5 \text{ nm} \times 1 \text{ nm}$ according to the exchange interaction length L_{ex} . In this essay, there will be 10×8 lines and each line with 100 cells (wire length/cell size). The resistance of each cell was expressed as

$$R_{i,\text{SV}} = R_{i,0} + 1/2 \times \Delta R_{i,\text{GMR}}^{\text{max}} (1 - m_{i,x-\text{PL}} m_{i,x-\text{FL}} - m_{i,y-\text{PL}} m_{i,y-\text{FL}}) + (\Delta R_{i,\text{AMR-PL}}^{\text{max}} + \Delta R_{i,\text{AMR-FL}}^{\text{max}}) \times \cos^2 (H_{\text{ext-}x} / H_{\text{ext}}) \quad (2)$$

where $R_{i,0}$ is the minimum overall resistance; $\Delta R_{i,\text{GMR}}^{\text{max}}$ is the maximum resistance variation of each cell brought by the GMR effect; $\Delta R_{i,\text{AMR-PL}}^{\text{max}}$ and $\Delta R_{i,\text{AMR-FL}}^{\text{max}}$ are the maximum resistance variations of each PL and FL cell brought by the AMR effect, respectively; $m_{i,x-\text{PL}}$, $m_{i,x-\text{FL}}$, $m_{i,y-\text{PL}}$, and $m_{i,y-\text{FL}}$ are normalized magnetization projections in x and y directions of the PL and FL layers respectively; H_{ext} and $H_{\text{ext-}x}$ are the applied magnetic field and the projection of it in the x direction. The equivalent resistance of SV was then computed taking the cells in the line as resistances in series and the lines as resistances in parallel.

It should be noted that the detailed computation method for the total resistance calculation in the SV stack is dependent on the relationship between the thickness t_{eff} (Fig. 1) and the exchange interaction length L_{ex} . When t_{eff} is smaller than L_{ex} , the cells with the same x and y value in the pinned layer should be taken as one cell and so are those in the free layer; then, the average value of their magnetizations is calculated. Otherwise, when the distance between the cell in PL and that in FL is smaller than L_{ex} , the corresponding resistances will be taken into

account as resistances in parallel. Then, the total resistance can be acquired. In this way, MR curves will be obtained with an external magnetic field sweeping of $-1592 \text{ kA/m} \rightarrow 1592 \text{ kA/m} \rightarrow -1592 \text{ kA/m}$.

4. Results and discussion

4.1. Giant magnetoresistance

The MR curve model was studied based on the nano-sized NiFe (3)/Cu (2)/CoFe (3) (in nm) SV-GMR stack when the external field was in the easy axis (y direction) and the exchange biasing field was 39.8 kA/m . In the simulation, $R_{i,0}$, MR, and $\Delta R_{i,\text{AMR}}^{\text{max}}$ were set as the experimental results, namely, 12.8Ω (corresponding to the thickness of 10 nm), 8.1% , and 0.1Ω , respectively, taking the geometrical factors into consideration.

It can be seen in Fig. 3 that the coercive field $\mu_0 H_c$ is 79.6 kA/m , which is larger than the experimental result probably due to the nanosize of the GMR stack. Moreover, the MR curve shape exhibits a good agreement with the experimental measurements. The differences between the simulated and the experimental curves can be attributed to the neglected surface roughness and thermal fluctuation effect, etc. The surface roughness has an influence on the spin valve properties, especially for the interfaces between the ferromagnetic layer and nonmagnetic layer, which can increase the spin dependent scattering. However, if the surface roughness is too great, the exchange biasing field and the reliability of SV-GMRs may be reduced. All the simulations were implemented at room temperature, but in fact, the temperature may not be uniform in the measurement.

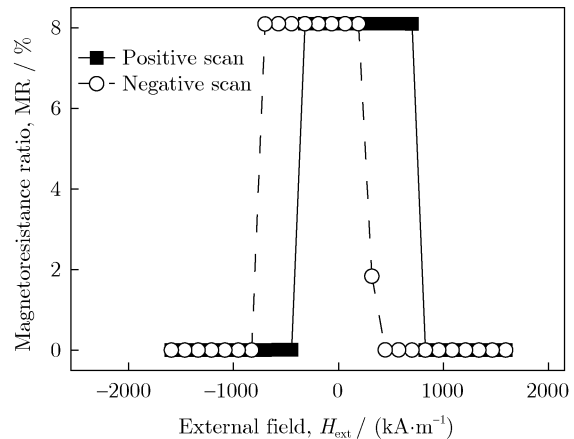


Fig. 3. Dependence of the magnetoresistance ratio MR on the external field H_{ext} ($\mu_0 H_{\text{bias}} = 39.8 \text{ kA/m}$, $J = -1.0 \times 10^{-3} \text{ J/m}^2$). Positive scan and negative scan represent the scanning from -1592 to 1592 kA/m and that from 1592 to -1592 kA/m , respectively.

4.2. Magnetization reversal

The hysteresis characteristics and magnetization re-

versals of the NiFe/Cu/CoFe SV were further investigated with different exchange coefficients. The magnetization variation mode is a jump variation mode raised from the jumps in the hysteresis cycles of NiFe/Cu/CoFe, whereas the hysteresis curve changes incrementally for NiFe/Cu/NiFe, which represents the incremental variation mode and is not described here. When the exchange coefficient is between -0.1×10^{-3} and $-0.6 \times 10^{-3} \text{J/m}^2$ (Fig. 4(a)), the magnetization reverses between NP and AP+ and PP states (Table 2) in the positive scan and then reverses between PP and AP- and NP states in the negative scan. When the exchange coefficient is $-0.8 \times$

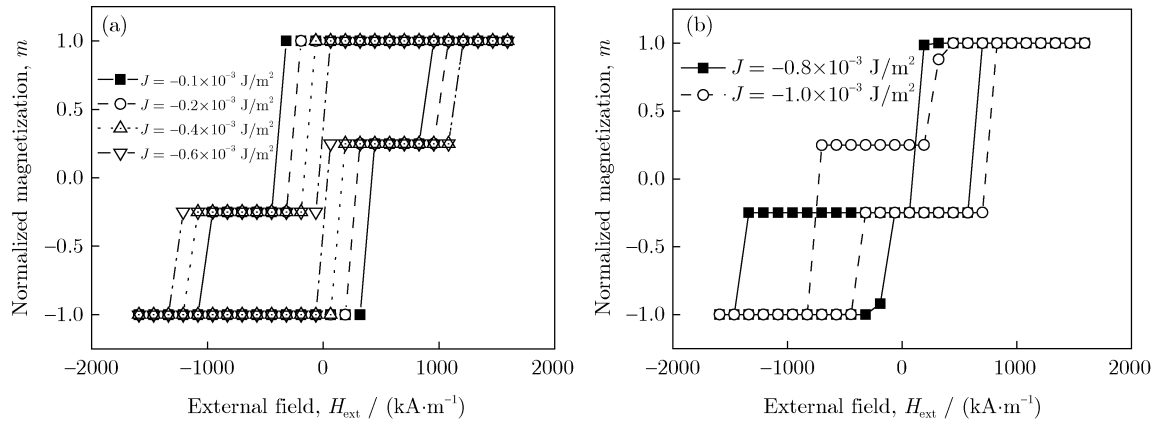


Fig. 4. Hysteresis cycles of NiFe (3)/Cu (2)/CoFe (3) (in nm) SV stack (the external field: y) with different exchange coefficients J .

Table 2. Different symbols which represent the magnetization directions of PL and FL

Magnetization direction	NP	AP-	AP+	PP
M_{PL}	Negative	Negative	Positive	Positive
M_{FL}	Negative	Positive	Negative	Positive

Further analysis into the magnetization reversal of the jump variation mode indicates that the magnetization distribution in the pinned layer rotates counterclockwise (CCW) from NP state to AP+ state, while that in the free layer rotates clockwise (CW) from AP+ state to PP state in the positive scan. The greater the absolute exchange coefficient is, the more difficult for the magnetizations of both the PL and FL to saturate. This phenomenon corresponds to the variation of energies: when the magnetization reverses from NP to AP+ state, the antiferromagnetic coupling energy and the demagnetizing energy decrease to the minimum value and remain unchanged until the magnetization reverses again from AP+ to PP. The six-neighboring exchange interaction energy decreases twice during the magnetization reversal. It can be inferred that the CCW and CW rotations are determined by the shape anisotropy and the antiferromagnetic coupling.

5. Conclusions

The magnetoresistance behavior and the magnetiza-

tion reversal mode in nanoscale spin valve giant magnetoresistance were investigated experimentally and theoretically with nanosized magnetic simulation methods. A NiFe/Cu/CoFe/IrMn SV-GMR structure was fabricated, and the MR value was measured to be 8.1% at room temperature. The simulated MR- H_{ext} shape agrees basically well with the experimental measurements and the differences between the simulated and experimental curves can be probably due to the neglecting of the surface roughness and thermal fluctuation effect. Moreover, the influence of the exchange coefficient on the magnetization reversal mode was studied. The reversal mode of the NiFe/Cu/CoFe/IrMn is a jump variation mode, and the switching field is almost linear with the exchange coefficient. Besides, further analysis of the magnetization reversal process reveals the variations of PL and FL, even those of the energies. The study can enrich the theoretical basis and analyzing means for nanosized GMRs, which will be valuable and helpful for the nanosized GMR sensor and magnetic random access memory (MRAM) application.

Acknowledgements

The authors are grateful to Professor Jin-liang He and Professor Jun Hu (Department of Electrical Engineering, Tsinghua University) for their suggestions and assis-

tance. This work was financially supported by the National Natural Science Foundation of China (Nos. 61025021 and 60936002), the National Key Project of Science and Technology of China (Nos. 2009ZX02023-001-3 and 2011ZX02403-002), and the Independent Scientific Research of Tsinghua University (No. 2010THZ0).

References

- [1] M.N. Baibich, J.M. Broto, A. Fert, F. Nguyen Van Dau, F. Petroff, P. Etienne, G. Creuzet, A. Friederich, and J. Chazelas, Giant magnetoresistance of (001)Fe/(001)Cr magnetic superlattices, *Phys. Rev. Lett.*, 61(1988), No. 21, p. 2472.
- [2] B. Dieny, V.S. Speriosu, S.S.P. Parkin, B.A. Gurney, D.R. Wilhoit, and D. Mauri, Giant magnetoresistive in soft ferromagnetic multilayers, *Phys. Rev. B*, 43(1991), No. 1, p. 1297.
- [3] K. Lee, M.J. Park, S. Lee, J.Y. Kim, and B.K. Cho, Spin-valve sensor with an out-of-plane magnetic anisotropy: for small field sensing applications, *J. Appl. Phys.*, 107(2010), No. 7, art. No. 073905.
- [4] R. Haraszczuk, S. Yamada, M. Kakikawa, and T. Ueno, Monitoring minute changes of magnetic markers' susceptibility by SV-GMR needle-type probe, *IEEE Trans. Magn.*, 47(2011), No. 10, p. 2584.
- [5] T.Q. Hung, S. Oh, J.R. Jeong, and C.G. Kim, Spin-valve planar Hall sensor for single bead detection, *Sens. Actuators A*, 157(2010), No. 1, p. 42.
- [6] K.M. Krishnan, Biomedical nanomagnetism: a spin through possibilities in imaging, diagnostics, and therapy, *IEEE Trans. Magn.*, 46(2010), No. 7, p. 2523.
- [7] A. Roldán, C. Reig, M.D. Cubells-beltrán, J.B. Roldán, D. Ramírez, S. Cardoso, and P.P. Freitas, Analytical compact modeling of GMR based current sensors: application to power measurement at the IC level, *Solid State Electron.*, 54(2010), No. 12, p. 1606.
- [8] Y. Yamagishi, S. Honda, J. Inoue, and H. Itoh, Numerical simulation of giant magnetoresistance in magnetic multilayers and granular films, *Phys. Rev. B*, 81(2010), No. 5, art. No. 054445.
- [9] S.X. She, D. Wei, Y. Zheng, B.J. Qu, T.L. Ren, X. Liu, and F.L. Wei, Micromagnetic simulation of transfer curve in giant-magnetoresistive head, *Chin. Phys. Lett.*, 26(2009), No. 12, art. No. 127503.
- [10] J.O. Oti, A general-purpose phenomenological micromagnetic model for modern giant magnetoresistive devices, *IEEE Trans. Magn.*, 46(2010), No. 6, p. 2338.
- [11] E.C. Stoner and E.P. Wohlfarth, A mechanism of magnetic hysteresis in heterogeneous alloys, *Philos. Trans. R. Soc. London Ser. A*, 240(1948), No. 826, p. 599.
- [12] H.R. Liu, *Study on Spin Valve Structure and GMR Sensor* [Dissertation], Tsinghua University, Beijing, 2006, p. 79.
- [13] OOMMF User's guide, 2004, <http://math.nist.gov/oommf/>.
- [14] C. Yin, Z. Jia, W.C. Ma, and T.L. Ren, Simulations of interaction among GMRs in a nano-sized biosensor array, *Tsinghua Sci. Technol.*, 16(2011), No. 2, p. 151.
- [15] L.D. Landau and E.M. Lifshitz, On the theory of the dispersion of magnetic permeability in ferromagnetic bodies, *Phys. Z. Sowjetunion*, 8(1935), p. 153.
- [16] R.A. Silva, T.S. Machado, G. Cernicchiaro, A.P. Guimarães, and L.C. Sampaio, Magnetoresistance and magnetization reversal of single Co nanowires, *Phys. Rev. B*, 79(2009), No. 13, art. No. 134434.
- [17] Z.M. Liao, Y. Lu, H.Z. Zhang, and D.P. Yu, Hysteresis magnetoresistance and micromagnetic modeling of Ni microbelts, *J. Magn. Magn. Mater.*, 322(2010), No. 15, p. 2231.